Quantum Phases in a Quantum Rabi Triangle

Yu-Yu Zhang,[1,2,*] Zi-Xiang Hu,[1,2] Libin Fu,[3] Hong-Gang Luo,[4] Han Pu,[5] and Xue-Feng Zhang (张学锋)[1,6,†]
[1]Department of Physics, Chongqing University, Chongqing 401330, China
[2]Chongqing Key Laboratory for strongly coupled Physics, Chongqing 401331, China
[3]Graduate School, China Academy of Engineering Physics, Beijing 100193, China
[4]School of Physical Science and Technology, Lanzhou University, Lanzhou 730000, China
[5]Department of Physics and Astronomy, and Rice Center for Quantum Materials, Rice University, Houston, Texas 77251-1892, USA
[6]Department of Physics, and Center of Quantum Materials and Devices, Chongqing University, Chongqing 401331, China

(Received 24 November 2020; accepted 30 June 2021; published 2 August 2021)

The interplay of interactions, symmetries, and gauge fields usually leads to intriguing quantum many-body phases. To explore the nature of emerging phases, we study a quantum Rabi triangle system as an elementary building block for synthesizing an artificial magnetic field. We develop an analytical approach to study the rich phase diagram and the associated quantum criticality. Of particular interest is the emergence of a chiral-coherent phase, which breaks both the $\mathbb{Z}_2$ and the chiral symmetry. In this chiral phase, photons flow unidirectionally and the chirality can be tuned by the artificial gauge field, exhibiting a signature of broken time-reversal symmetry. The finite-frequency scaling analysis further confirms the associated phase transition to be in the universality class of the Dicke model. This model can simulate a broad range of physical phenomena of light-matter coupling systems, and may have an application in future developments of various quantum information technologies.

DOI: 10.1103/PhysRevLett.127.063602

Introduction.—The coupling between light and matter has brought forth a novel class of quantum many-body systems [1–5], which is useful in probing a broad range of physical phenomena. The possibility of quantum phase transition (QPT) of photons has stimulated a lot of discussions in the Jaynes-Cummings (JC) Hubbard lattice [6–8] and the Rabi lattice models [9–11]. The basic building block of such systems contains a two-level system and a bosonic field mode, which is the simplest and the most fundamental model describing quantum light-matter interactions [12,13]. Usually, the QPTs are discussed in the thermodynamical limit [14]. However, the quantum Rabi model [15–18], two-site JC lattice [19], and few-body systems with nonlinearity [20] in proper limits also exhibit the similar scaling behavior of QPTs. Such QPTs in a few-body system open a window for investigating related integrability, exotic phases, and critical behaviors [15–17,21,22].

The intriguing many-body phases generally arise from the interplay of strong interactions, symmetries, and external fields. In recent years artificial gauge fields have been created for quantum platforms with bosonic excitations, such as neutral atomic Bose-Einstein condensate (BEC) or cold quantum gases [23–25], and photonic systems [26–30]. For example, manifestations of artificial magnetism in quantum gases in terms of vortex nucleation have been found [24], the intriguing phenomenon of fractional quantum Hall (FQHE) physics has been predicted to occur in the JC Hubbard system by applying an artificial magnetic field [31–33]. A few-body system of light-atom interactions subjected to an artificial magnetic field provides an ideal platform to investigate new quantum phases, which can be controlled conveniently by the artificial gauge fields.

In this Letter, we study the quantum Rabi triangle (QRT), as a fundamental unit for synthesizing a magnetic field to manipulate photons in optical cavities, to explore the possibility of phase transitions in a few-body system. Mean-field approximations are usually adopted in many-body systems and often yield quantitatively accurate results. This, however, is in general no longer true in dealing with few-body systems. As such, analytic results can rarely be found in few-body systems. Remarkably, we show that exact analytic results can be found in the QRT in the infinite frequency limit (analogous to the thermodynamic limit). Using this analytic approach, we construct the phase diagram of the QRT and explore the associated phase transitions. The QRT contains three phases. An incoherent phase (iCP), analogous to the normal phase in the Dicke model, dominates the weak coupling regime. In the strong coupling regime, there exist two coherent phases: the normal coherent phase (nCP) is analogous to the superradiance phase in the Dicke model and breaks the $\mathbb{Z}_2$ symmetry; the chiral coherent phase (cCP) breaks both the $\mathbb{Z}_2$ and the chiral symmetry and is unique to the QRT without analogy in the Dicke model. The transition between nCP and cCP is of first order and can be induced by adjusting the artificial gauge field. The transition

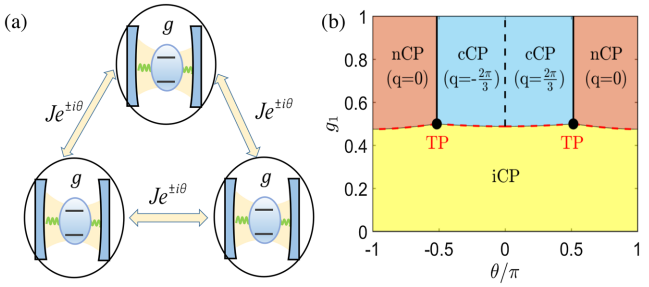

FIG. 1. (a) The schematic diagram of quantum Rabi triangle system with artificial gauge field. (b) The analytic phase diagram in the g_1-θ parameter space. The second order critical lines (red dash) from the iCP to nCP and cCP join with the first order line (black sold) between nCP and cCP at the triple points (TPs) (black dot). The black dashed line separates the cCP according to its chirality. In all our calculations, we set $\omega = 1$ as the units for frequency, and $\Delta = 50$, $J = 0.05$.

between iCP and the two coherent phases is of second-order and, through a finite-frequency scaling, can be shown to belong to the same universality class of the superradiance phase transition in the Dicke model.

Model.—The QRT is a model of itinerant photons hopping between neighboring cavities and interacting on-site with a two-level atom. Three cavities are placed on a ring, see Fig. 1(a), where each cavity contains a two-level atom and is described by the quantum Rabi model. The full Hamiltonian for the QRT system reads

$$H_{\mathrm{QRT}} = \sum_{n=1}^{3} H_{R,n} + \sum_{n,n'}^{3} J(e^{i\theta} a_n^\dagger a_{n'} + e^{-i\theta} a_n a_{n'}^\dagger), \quad (1)$$

where $a_n^\dagger$ (a_n) is the photonic creation (annihilation) operator of the nth cavity with frequency ω, $Je^{\pm i\theta}$ is the hopping amplitude between cavities n and n', and $H_{R,n}$ denotes the quantum Rabi model of the nth cavity

$$H_{R,n} = \omega a_n^\dagger a_n + g(a_n^\dagger + a_n)\sigma_n^x + \frac{\Delta}{2}\sigma_n^z, \quad (2)$$

with $\vec{\sigma}_n = \{\sigma_n^x, \sigma_n^y, \sigma_n^z\}$ the Pauli matrix describes the two-level atom with energy gap Δ and g denotes the strength of cavity-atom coupling. The nonzero static phase θ in the photon hopping amplitude arises from an artificial gauge field $A_{n,n'}$ as $\theta = \int_{r_n}^{r_{n'}} A(r)dr$ [31,32]. The gauge-invariant effective magnetic flux in the ring is $\phi = 3\theta$. This artificial gauge field can be realized by a periodic modulation of the photon hopping strength between cavities, the details of which can be found in the Supplemental Material [34]. We will focus on the infinite-frequency limit, in which Δ is much larger than any other frequency scales in the system. This is the limit where the single-cavity Rabi model also exhibits the superradiance phase transition [15–17,35] as in the Dicke model.

Similar to the Rabi model, the parity operator can be defined as $\hat{P} = \prod_n \exp(i\pi \hat{N}_n)$, where $\hat{N}_n = a_n^\dagger a_n + \sigma_n^+ \sigma_n^-$ is the number of excitation quanta of the nth cavity. Because $[H_{\mathrm{QRT}}, \hat{P}] = 0$, the parity operator $\hat{P}$ is conserved and equal to ± 1, depending on whether the total number of excitation quanta is even or odd. Besides such $\mathbb{Z}_2$ symmetry, the time-reversal symmetry (TRS) of hopping processes among three cavities is artificially broken when $\theta \neq m\pi (m \in \mathbb{Z})$. However, it can be recovered by implementing the chiral transformation C_r which exchange the even and odd permutation ($123 \leftrightarrow 321$). Considering that the gauge field plays a critical role in the search for exotic quantum phases of matter, it can be anticipated that it will give rise to interesting properties in the QRT system. In Fig. 1(b), we plot the phase diagram in the parameter space spanned by g_1 and θ, where $g_1 = g/\sqrt{\Delta\omega}$ is the scaled dimensionless coupling strength, and θ is restricted between $-\pi$ and π. We will now discuss the three phases in detail.

Incoherent phase.—In the weak coupling regime (i.e., small g_1), the number of excitations tends to zero and no photon propagates in the cavities, and we have the so-called incoherent phase (iCP). To obtain its energy spectrum, we first implement the Schrieffer-Wolff transformation with the unitary operator $S_n = \exp[-ig_1\sqrt{\omega/\Delta}\sigma_n^y(a_n^\dagger + a_n)]$ on each cavity. After neglecting higher-order terms in the limit $\Delta/\omega \to \infty$, Hamiltonian (1) becomes

$$H_{\mathrm{iCP}} = \sum_{n=1}^{3} \omega a_n^\dagger a_n + \frac{\Delta}{2}\sigma_n^z + \omega g_1^2 (a_n + a_n^\dagger)^2 \sigma_n^z + J(e^{i\theta} a_n^\dagger a_{n+1} + \mathrm{H.c.}) + O\left(g_1^4 \frac{\omega^2}{\Delta^2}\right). \quad (3)$$

Because the transverse operator σ_n^x is eliminated, the two atomic levels are decoupled. Thus, the low-energy effective Hamiltonian can be obtained by projecting to the subspace of the lower atomic level $|\downarrow\rangle_n$, i.e., $H_{\mathrm{iCP}}^{\downarrow} = \langle\downarrow|H_{\mathrm{iCP}}|\downarrow\rangle$. After taking a discrete Fourier transform $a_n^\dagger = (1/\sqrt{N})\sum_q e^{inq} a_q^\dagger$ with the quasimomentum q taking values 0 and $\pm 2\pi/3$, we have

$$H_{\mathrm{iCP}}^{\downarrow} = E_0 + \sum_q \omega_q a_q^\dagger a_q - \omega g_1^2 (a_q a_{-q} + a_q^\dagger a_{-q}^\dagger), \quad (4)$$

where $E_0 = -3\Delta/2 - 3\omega g_1^2 + 3(\omega + J)g_1^2\omega/\Delta$ is a constant, and $\omega_q = \omega - 2\omega g_1^2 + 2J\cos(\theta - q)$ (see Supplemental Material [34]). Hamiltonian (4) is quadratic in photon operators and hence can be diagonalized using the Bogoliubov transformation [34]. The diagonalized Hamiltonian takes the form $H_{\mathrm{iCP}}^{\downarrow} = \sum_q \varepsilon_q a_q^\dagger a_q + E_g$,

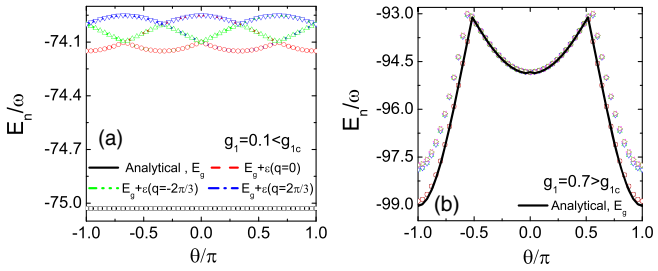

FIG. 2. (a) Energy spectrum in the iCP phase with $g_1 = 0.1$. Curves represent the analytic result. Symbols correspond to the lowest 4 eigenenergies numerically obtained from ED. (b) Energy spectrum in the nCP and cCP phases with $g_1 = 0.7$. The black curve corresponds to analytic ground-state energy. Symbols correspond to the lowest 6 eigenenergies numerically obtained from ED. Other parameters are the same as in Fig. 1. The two peaks are located at $\pm\theta_c = \pm 0.516\pi$.

where $E_g = \sum_q(\varepsilon_q - \omega_q)/2 + E_0$ is the ground-state energy, and the photon dispersion is given by

$$\varepsilon_q = \frac{1}{2}[\sqrt{(\omega_q + \omega_{-q})^2 - 16\omega^2 {g_1}^4} + \omega_q - \omega_{-q}]. \quad (5)$$

The excitation spectra ε_q with the momentum $q = 0, \pm 2\pi/3$ decreases to zero as the coupling strength increases to a critical value (see Fig. 1 in the Supplemental Material [34]).

Figure 2(a) shows the analytical ground-state energy and the first few excited-state energies for the iCP phase, which agree well with numerical results obtained from exact diagonalization (ED) of the original Hamiltonian (1). It is observed that the iCP is a gapped phase with nondegenerate ground state and there exist energy-level crossings in excited states. It should be noted that the ground state has even parity. This can be understood from the fact that at $g_1 = 0$, there are no photons and all the atoms are in the lower level $|\downarrow\rangle$ in the ground state, which clearly has an even excitation number 0.

Coherent phases.—In the strong coupling regime, there exist two coherent phases, in which the cavity field is macroscopically populated [15]. To obtain the effective Hamiltonian, we first shift the cavity operator as $a_n \to a_n + \alpha_n$ with the complex displacement α_n. With the displaced operator, the QRT Hamiltonian takes the form

$$H_{\mathrm{CP}} = \sum_n \omega a_n^\dagger a_n + \frac{\Delta_n'}{2}\tau_n^z + g_n'(a_n^\dagger + a_n)\tau_n^x + J a_n^\dagger(e^{i\theta}a_{n+1} + e^{-i\theta}a_{n-1}) + V_{\mathrm{off}} + E_0, \quad (6)$$

where $\Delta_n' = \sqrt{\Delta^2 + 16g^2A_n^2}$ is the renormalized energy gap, and $g_n' = g\Delta/\Delta_n'$ the effective coupling strength. Here, $\tau_n^z = \Delta/\Delta_n'\sigma_n^z + 4gA_n/\Delta_n'\sigma_n^x$ is the transformed Pauli matrix. The off-diagonal term V_{off} and the energy constant E_0 are given in the Supplemental Material [34]. A proper choice of the displacement α_n leads to the vanish of V_{off} and, as a result, Hamiltonian (6) has the same structure as Hamiltonian (1) with the rescaled frequency Δ_n' and coupling strength g_n'. Therefore, by employing the same procedure used to derive H_{iCP}, we obtain the effective Hamiltonian in the coherent phases by projecting to the spin subspace $|\downarrow\rangle$

$$H_{\mathrm{CP}}^{\downarrow} = \sum_{n=1}^{3} \omega a_n^\dagger a_n - \frac{g_n'^2}{\Delta_n'}(a_n^\dagger + a_n)^2 - \frac{\Delta_n'}{2} + J a_n^\dagger(e^{i\theta}a_{n+1} + e^{-i\theta}a_{n-1}) + E_0. \quad (7)$$

Diagonalizing the above quadratic Hamiltonian, we obtain two coherent phases [see Fig. 1(b)]: (i) *normal-coherent phase (nCP):* The nCP occurs for $|\theta| > \theta_c$, where θ_c is a critical value for the phase of the photon hopping amplitude (see below). In the nCP, the ground state features $q = 0$, which indicates that photons have zero quasimomentum, and α_n can be taken to be real with the explicit expression [34] $\alpha_n = \sqrt{[g^2/(\omega + 2J\cos\theta)^2] - (\Delta/4g)^2}$ independent of n. The photon dispersion is given by

$$\varepsilon_q = \frac{1}{2}(\omega_q' - \omega_{-q}') + \sqrt{(\omega_q' + \omega_{-q}')^2 - 16g_n'^4/\Delta_n'^2}, \quad (8)$$

where $\omega_q' = \omega - 2g_n'^2/\Delta_n' + 2J\cos(\theta - q)$. Furthermore, the ground state is twofold degenerate as a result of the $\mathbb{Z}_2$ symmetry breaking. This twofold degeneracy can be seen from the ED numerical results presented in Fig. 2(b), where the left and right parts of the curve represent the nCP. In Fig. 3(a) we show how the order parameters $\langle a_n\rangle$ vary as a function of the coupling strength g_1. In increasing g_1, the system enters from the iCP (where $\langle a_n\rangle = 0$) to the nCP, and the order parameter grows from zero, indicating a second-order phase transition. In nCP, $\langle a_n\rangle$ are the same for all three cavities. Figure 3(a) only shows one of the two degenerate ground-state solutions for nCP. The order parameter takes a minus sign in the other solution. (ii) *chiral-coherent phase (cCP):* The cCP, which occurs when $|\theta| < \theta_c$, features finite photon quasimomentum $q = \pm 2\pi/3$. Here the displacement α_n is in general complex and n dependent. The middle part of Fig. 2(b) between the two cusps, denoting the position of $\pm\theta_c$, represents the ground-state energy of cCP. The ED results also clearly show that the ground state has sixfold degeneracy. This is because, in addition to the $\mathbb{Z}_2$ symmetry, the cCP also breaks the chiral symmetry resulting in a unidirectional photon current. Figure 3(b) shows how the magnitude of the order parameter vs g_1 when the system enters from iCP to cCP. One can again see a second-order phase transition. However, different from nCP, the order parameters in cCP are n dependent and are, in general, complex. For the example shown in the figure, the phase angles for $\langle a_{1,2,3}\rangle$

are π, -0.11126 and 0.11126, respectively, and are nearly insensitive to the value of g_1. Here we only show one of the six degenerate ground-state solutions. In the other solutions, the order parameters take cyclic permutations and/or take a minus sign. To better characterize the photon current and the chirality, we define the photon current operator as $I_{\rm ph} = i[(a_1^\dagger a_2 + a_2^\dagger a_3 + a_3^\dagger a_1) - \text{H.c.}]$, analogous to the continuity equation in classical systems. Moreover, in analogy with the spin chiral operator via Pauli matrix $C = \frac{1}{2}\sum_{<ijk>} \vec{\sigma}_i \cdot (\vec{\sigma}_j \times \vec{\sigma}_k)$ [36], the photon chiral operator can be defined as $C_{\rm ph} = -2i \sum_{<ijk>} \varepsilon_{ijk} a_i a_j^\dagger (n_k - 1/2)$ (ε_{ijk} is Levi-Civita tensor) with help of the linearized spin-wave transformation $\sigma_i^- = a_i$, $\sigma_i^+ = a_i^\dagger$ and $\sigma_i^z = 2a_i^\dagger a_i - 1$ [9,37]. Similar to the spin system, the photon chiral operator is odd under either the chiral transformation $C_r^{-1} C_{\rm ph} C_r = -C_{\rm ph}$, or the TRS transformation. Meanwhile, the photon current operator has the same properties of the symmetries. In Figs. 3(c) and 3(d), we show $I_{\rm ph}$ and $C_{\rm ph}$, respectively, as functions of θ. One can see that these two quantities are zero for nCP and finite for cCP, except at $\theta = 0$, where TRS is recovered in the Hamiltonian.

Quantum criticality and phase boundaries.—As mentioned above, the transition from the iCP to either coherent phases is of second order and is induced by varying the coupling strength g_1. The critical coupling strength g_{1c} can be obtained from the excitation spectra ε_q in Eq. (5)—ε_q must vanish at g_{1c}, yielding

$$g_{1c}(q) = \sqrt{\frac{1 + (4J/\omega)\cos\theta\cos q + (4J^2/\omega^2)\cos(\theta+q)\cos(\theta-q)}{4[1 + (2J/\omega)\cos\theta\cos q]}}. \tag{9}$$

The transition between the two coherent phases, by contrast, is of first order, features discontinuous jump in the order parameter, and is induced by varying the effective magnetic flux θ. Using the analytic expressions of the ground-state energy for nCP and cCP, we obtain the critical value θ_c as [34]

$$\theta_c = \cos^{-1}\left(-\frac{2J}{\sqrt{8J^2 + \omega^2} + \omega}\right), \tag{10}$$

and the phase boundary between nCP and cCP occurs at $\pm\theta_c$. Note that θ_c is independent of g_1.

These results allow us to construct the phase diagram presented in Fig. 1(b). There are two triple points (TPs) in the phase diagram, at which all three phases coexist. The TPs are located at $(g_{tc}, \pm\theta_c)$ where the value of g_{tc} can be obtain from $g_{1c}(q = 0) = g_{1c}(q = \pm 2\pi/3)$, which yields

$$g_{tc} = \frac{1}{2}\sqrt{\frac{3}{2} - \frac{\sqrt{8J^2 + \omega^2}}{2\omega}}. \tag{11}$$

Universal scaling.—The QRT Hamiltonian can exhibit a scaling relation for finite values of Δ/ω as a consequence of continuous QPTs in the thermodynamic limit. The universal scaling of the QPTs can be characterized by the critical exponents for finite values of $\eta = \Delta/\omega$. Figure 4 illustrates the finite-η scaling of the ground-state energy and the average photon number obtained by numerical diagonalization in the critical regime. In the limit $\eta \to \infty$, the scaled ground-state energy E_g/η obtained analytically at the critical point approaches $c_0 = -3\omega/2$. To show the leading finite-η corrections, we calculate $E_g/\eta - c_0$ versus η at the critical value g_{1c} on a log-log scale in Fig. 4(a) when the system undergoes the iCP-cCP QPT with $\theta = 1.2\theta_c$ and the iCP-nCP QPT with $\theta = 0.96\theta_c$, respectively. The corresponding slope of the curves in the large-η regime gives a universal exponent -1 for both QPTs. Meanwhile, a power-law behavior of the photon number $N_p = \sum_n \langle a_n^\dagger a_n \rangle$ exists at large η as shown in Fig. 4(b). The corresponding finite-η exponent extracted from the curves converges to -0.667 as shown in the inset. To conclude, we find that the scaling exponents for the ground-state energy and the average photons number are universal, giving two

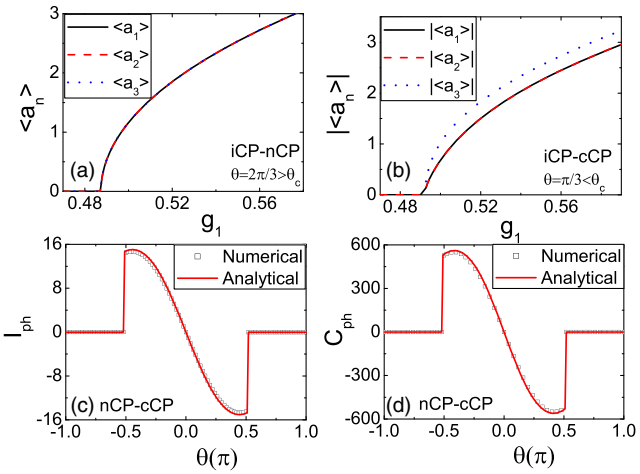

FIG. 3. (a) The order parameter $\langle a_n \rangle$ as a function of the scaled coupling strength g_1 for the iCP-nCP transition with $\theta = 2\pi/3 > \theta_c$. (b) $|\langle a_n \rangle|$ as a function of g_1 for the iCP-cCP transition with $\theta = \pi/3 < \theta_c$. (c) Photon current $I_{\rm ph}$ and (d) the expected value of the chirality operator $C_{\rm ph}$ in the ground state as a function of the hopping phase θ for the nCP-cCP transition with $g_1 = 0.7 > g_{1c}$. Other parameters are the same as in Fig. 1.

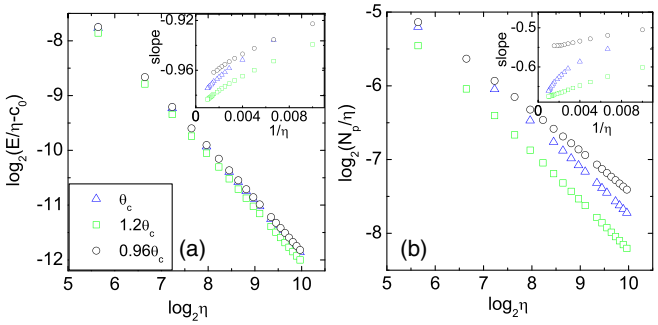

FIG. 4. Scaling of the ground-state energy (a) and photon number (b) as a function of η at the critical point for the different gauge field phases $\theta = \theta_c$, $1.2\theta_c$, and $0.96\theta_c$ for continuous QPTs of the iCP-nCp and iCP-cCP transitions. The insets show the corresponding slope versus $1/\eta$.

power law expressions as $E_g/\eta - c_0 \propto \eta^{-1}$ and $N_p/\eta \propto \eta^{-2/3}$ for both the iCP-nCP and the iCP-cCP transitions, belonging to the same universality class of the Dicke model [38,39] and the single-site Rabi model in the infinite-frequency limit [15,16].

Conclusion–We present an exact analytic solution to the quantum Rabi triangle system as a basic building block for exploring strongly correlated physical phenomena. We identify the quantum phases and the transitions among them. In particular, there is an exotic chiral coherent phase that has no analog in the single-cavity Dicke or Rabi models. The cCP breaks both the $\mathbb{Z}_2$ and the chiral symmetry, featuring a persistent unidirectional photon current in its ground state. The current and the chirality can be tuned by the phase of the intercavity photon hopping amplitude, which plays the role of an artificial magnetic flux.

Our study advances the field of strongly correlated photons in a light-atom coupled system. Studying the quantum phases in this few-body system under the introduction of an artificial magnetic field would open intriguing avenues for exploring their connection to strongly correlated photons in two-dimensional lattice systems [9–11]. Moreover, an implementation of the system considered in this Letter is an exciting prospect for the future and may be applicable in future developments of various quantum information technologies. One has proposed an application of the Mott state in the JC Hubbard lattice for implementing quantum information processing [33]. One could hope to implement cluster state quantum computing related to extension of the quantum Rabi triangle system coupled to many resonators for strong atom-resonator coupling. Our studies also shed new light on quantum simulation of artificial magnetic fields in ultracold bosonic atoms [24].

The authors thank Qing-Hu Chen for useful discussions. This work was supported by NSFC under Grants No. 12075040, No. 11804034, No. 11874094, No. 12047564, No. 11834005, No. 11974064, No. 11725417, No. 12088101, and No. 12047501, NSAF under Grant No. U1930403, and Chongqing NSF under Grants No. cstc2020jcyj-msxmX0890 and No. cstc2018jcyjAX0399, Fundamental Research Funds for the Central Universities Grants No. 2020CDJQY-Z003 and No. 2021CDJQY-007. H. P. acknowledges support from the U.S. NSF and the Welch Foundation (Grant No. C-1669).

*yuyuzh@cqu.edu.cn
†zhangxf@cqu.edu.cn

[1] T. Niemczyk, F. Deppe, H. Huebl, E. P. Menzel, F. Hocke, M. J. Schwarz, J. J. Garcia-Ripoll, D. Zueco, T. Hümmer, E. Solano, A. Marx, and R. Gross, Nat. Phys. **6**, 772 (2010).
[2] P. Forn-DÍaz, J. J. GarcÍa-Ripoll, B. Peropadre, J.-L. Orgiazzi, M. A. Yurtalan, R. Belyansky, C. M. Wilson, and A. Lupascu, Nat. Phys. **13**, 39 (2017).
[3] F. Yoshihara, T. Fuse, S. Ashhab, K. Kakuyanagi, S. Saito, and K. Semba, Nat. Phys. **13**, 44 (2017).
[4] P. Pippan, H. G. Evertz, and M. Hohenadler, Phys. Rev. A **80**, 033612 (2009).
[5] I. Bloch, J. Dalibard, and W. Zwerger, Rev. Mod. Phys. **80**, 885 (2008).
[6] M. J. Hartmann, F. G. S. L. Brando, and M. B. Plenio, Nat. Phys. **2**, 849 (2006).
[7] A. D. Greentree, C. Tahan, J. H. Cole, and L. C. Hollenberg, Nat. Phys. **2**, 856 (2006).
[8] G. Zhu, S. Schmidt, and J. Koch, New J. Phys. **15**, 115002 (2013).
[9] H. Zheng and Y. Takada, Phys. Rev. A **84**, 043819 (2011).
[10] M. Schiró, M. Bordyuh, B. Öztop, and H. E. Türeci, Phys. Rev. Lett. **109**, 053601 (2012).
[11] T. Flottat, F. Hébert, V. G. Rousseau, and G. G. Batrouni, Eur. Phys. J. D **70**, 213 (2016).
[12] I. I. Rabi, Phys. Rev. **51**, 652 (1937).
[13] P. Forn-Diaz, L. Lamata, E. Rico, J. Kono, and E. Solano, Rev. Mod. Phys. **91**, 025005 (2019).
[14] S. Sachdev, *Quantum Phase Transitions* (Cambridge University Press, Cambridge, England, 1999).
[15] M. J. Hwang, R. Puebla, and M. B. Plenio, Phys. Rev. Lett. **115**, 180404 (2015).
[16] M. X. Liu, S. Chesi, Z.-J. Ying, X. Chen, H.-G. Luo, and H.-Q. Lin, Phys. Rev. Lett. **119**, 220601 (2017).
[17] X. Y. Chen, Y. Y. Zhang, L. B. Fu, and H. Zheng, Phys. Rev. A **101**, 033827 (2020).
[18] X. Y. Lü, L. L. Zheng, G. L. Zhu, and Y. Wu, Phys. Rev. Applied **9**, 064006 (2018).
[19] M. J. Hwang and M. B. Plenio, Phys. Rev. Lett. **117**, 123602 (2016).
[20] S. Felicetti and A. Le Boité, Phys. Rev. Lett. **124**, 040404 (2020).
[21] D. Braak, Phys. Rev. Lett. **107**, 100401 (2011).
[22] Q. H. Chen, C. Wang, S. He, T. Liu, and K. L. Wang, Phys. Rev. A **86**, 023822 (2012).
[23] Y. J. Lin, R. L. Compton, K. Jiménez-García, J. V. Porto, and I. B. Spielman, Nature (London) **462**, 628 (2009).

[24] J. Dalibard, F. Gerbier, G. Juzeliūnas, and P. Öhberg, Rev. Mod. Phys. **83**, 1523 (2011).
[25] H. Cao, Q. Wang, and L. B. Fu, Phys. Rev. A **89**, 013610 (2014).
[26] R. O. Umucalilar and I. Carusotto, Phys. Rev. Lett. **108**, 206809 (2012).
[27] D. W. Wang, H. Cai, R. B. Liu, and M. O. Scully, Phys. Rev. Lett. **116**, 220502 (2016).
[28] H. Cai and D. W. Wang, Natl. Sci. Rev. **8**, 196 (2021).
[29] P. Roushan *et al.*, Nat. Phys. **13**, 146 (2017).
[30] I. Bloch, J. Dalibard, and S. Nascimbene, Nat. Phys. **8**, 267 (2012).
[31] A. L. C. Hayward, A. M. Martin, and A. D. Greentree, Phys. Rev. Lett. **108**, 223602 (2012).
[32] A. L. C. Hayward and A. M. Martin, Phys. Rev. A **93**, 023828 (2016).
[33] C. Noh and D. G. Angelakis, Rep. Prog. Phys. **80**, 016401 (2017).
[34] See Supplemental Material at http://link.aps.org/supplemental/10.1103/PhysRevLett.127.063602 for more details about the calculation.
[35] M.-L. Cai, Z.-D. Liu, W.-D. Zhao, Y.-K. Wu, Q.-X. Mei, Y. Jiang, L. He, X. Zhang, Z.-C. Zhou, and L.-M. Duan, Nat. Commun. **12**, 1126 (2021).
[36] X. G. Wen, F. Wilczek, and A. Zee, Phys. Rev. B **39**, 11413 (1989).
[37] D. C. Mattis, *The Theory of Magnetism* (Springer, Berlin, 1988).
[38] N. Lambert, C. Emary, and T. Brandes, Phys. Rev. Lett. **92**, 073602 (2004).
[39] Q. H. Chen, Y. Y. Zhang, T. Liu, and K. L. Wang, Phys. Rev. A **78**, 051801(R) (2008).